Supporting Information

Quantification of Nitrite in Beverages and Pickled Foods with a High-Sensitivity Amperometric Biosensor Enhanced by a Multilayer Perceptron Neural Network

Zhongwei Liang[a], Guang Yang[a], Zidong Chen[a], Bingxin Zhong[a], Bin Ran[b], Bo Liu[c], Jialin Liang[d], Teng Shen[a], Peng Liu[e], Daqi Chen[a,*], Chaozhan Chen[a,*]

[a] School of Mechanical and Electrical Engineering, Guangzhou University, Guangzhou 518055, PR China

[b] School of Science, Harbin Institute of Technology, Shenzhen, Shenzhen 518055, PR China

[c] School of Energy and Power Engineering, Shandong University, Jinan 250061, China

[d] School of Energy and Power Engineering, Beijing Institute of Technology, Zhuhai, Zhuhai 519088, China

[e] School of Chemistry and Chemical Engineering, Guangzhou University, Guangzhou 518055, PR China

[*] Corresponding author: Chaozhan Chen, Daqi Chen

E-mail address: chaozhanchen@foxmail.com, daqichen@gzhu.edu.cn

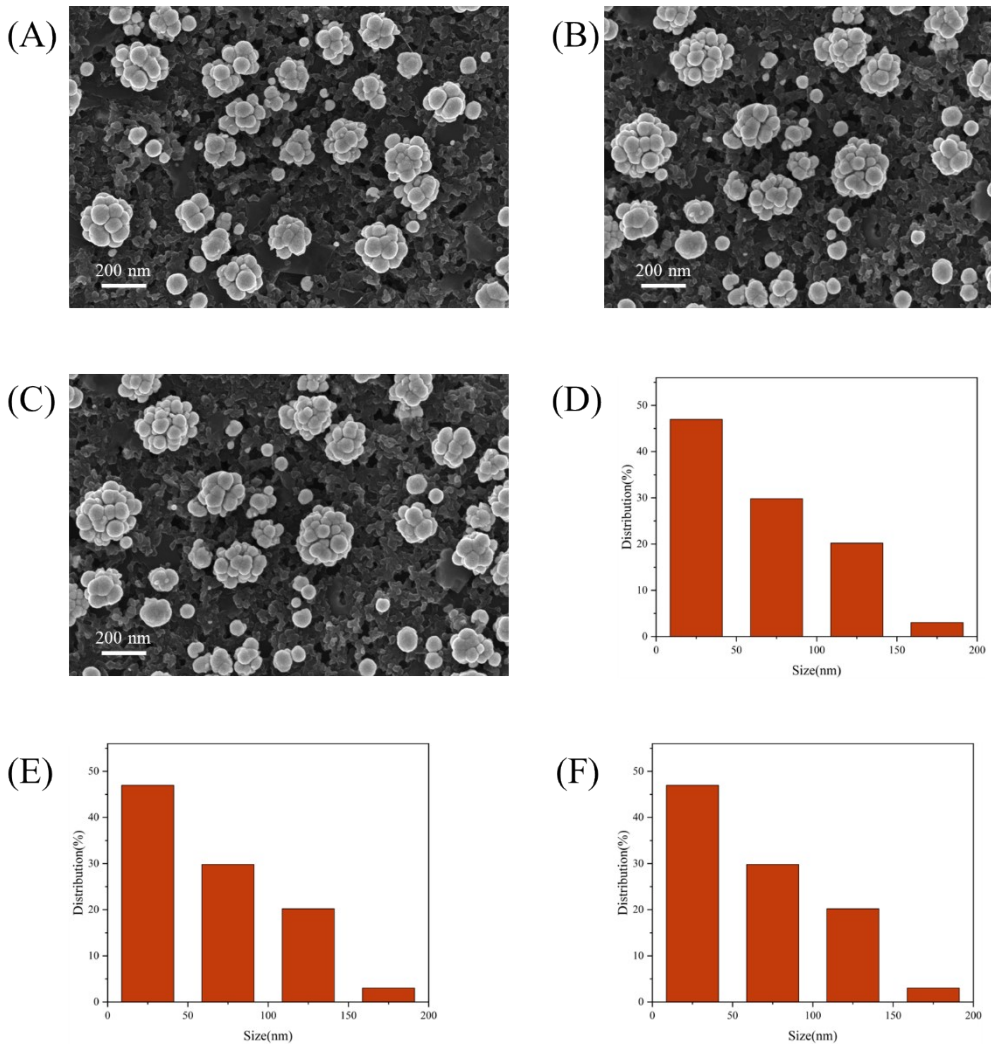

Fig. S1. (A–C) Representative SEM images taken from three different regions of the Pt–Cu/Au/SPE surface. (D–F) Corresponding nanoparticle size distribution histograms for (A–C).

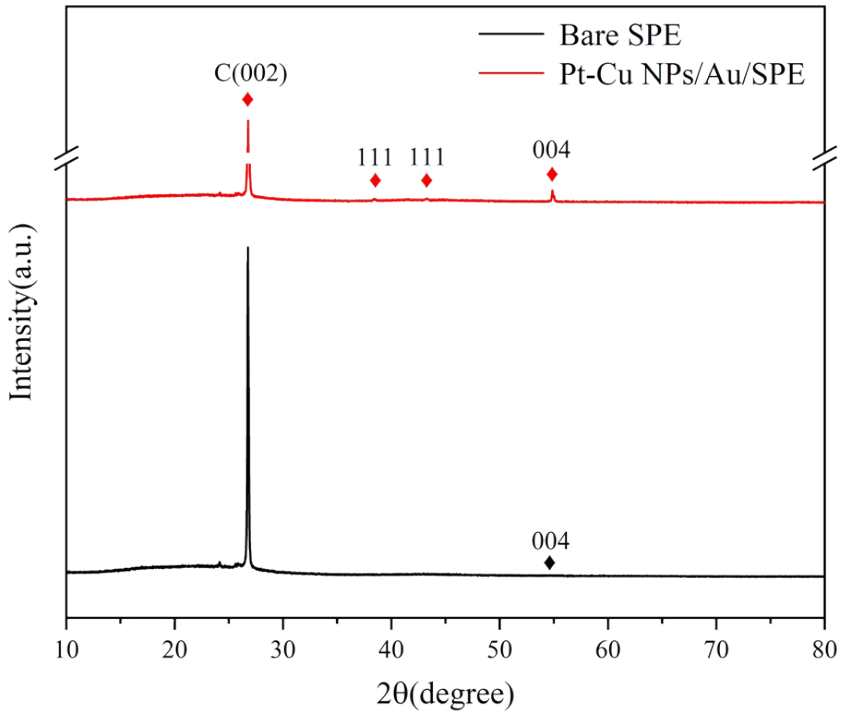

Fig. S2 X-ray diffraction patterns of bare SPE and Pt-Cu NPs/Au NPs/SPE.

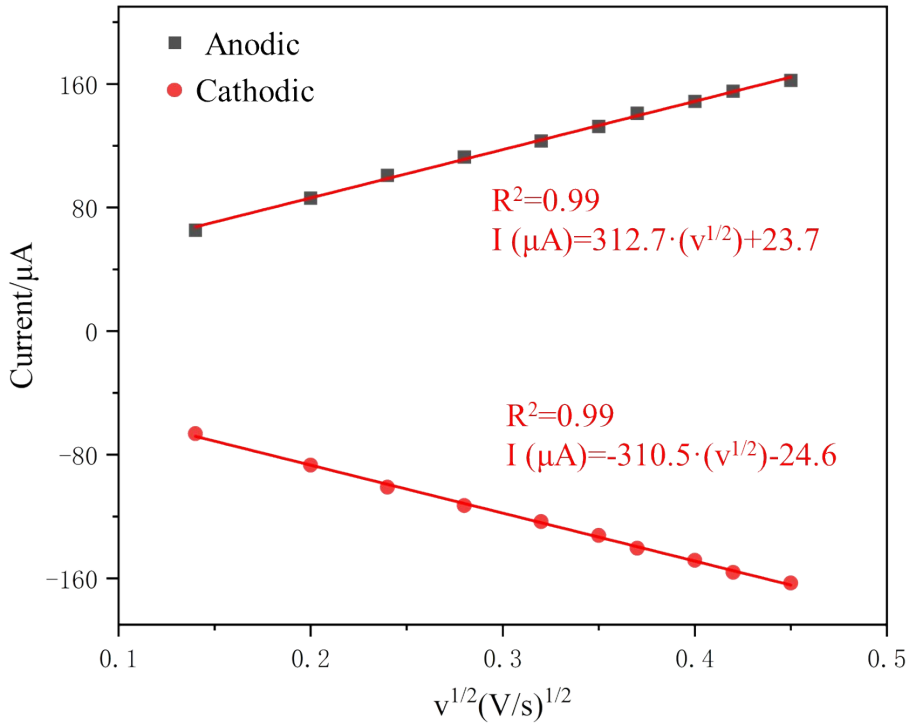

Fig. S3 The relationship between the square root of the scan rate and peak current for Pt-Cu NPs/Au/SPE.

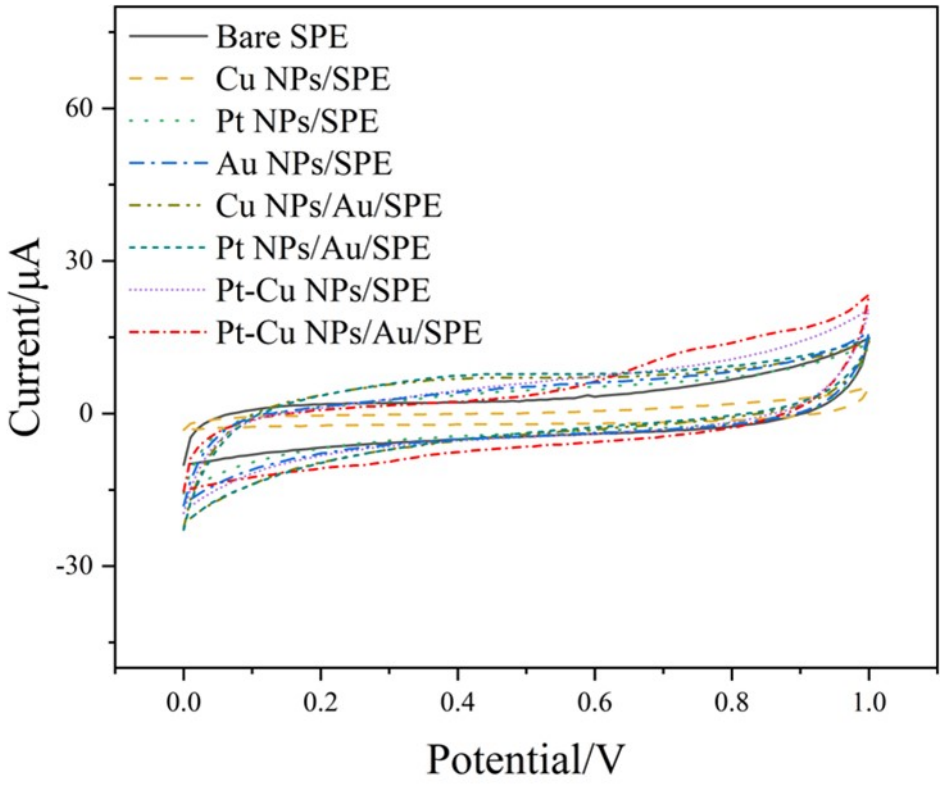

Fig. S4 CVs of bare SPE, Cu NPs/SPE, Pt NPs/SPE, Au NPs/SPE, Cu NPs/Au/SPE, Pt NPs/Au/SPE, Pt-Cu NPs/SPE and Pt-Cu NPs/Au/SPE in PBS solution.

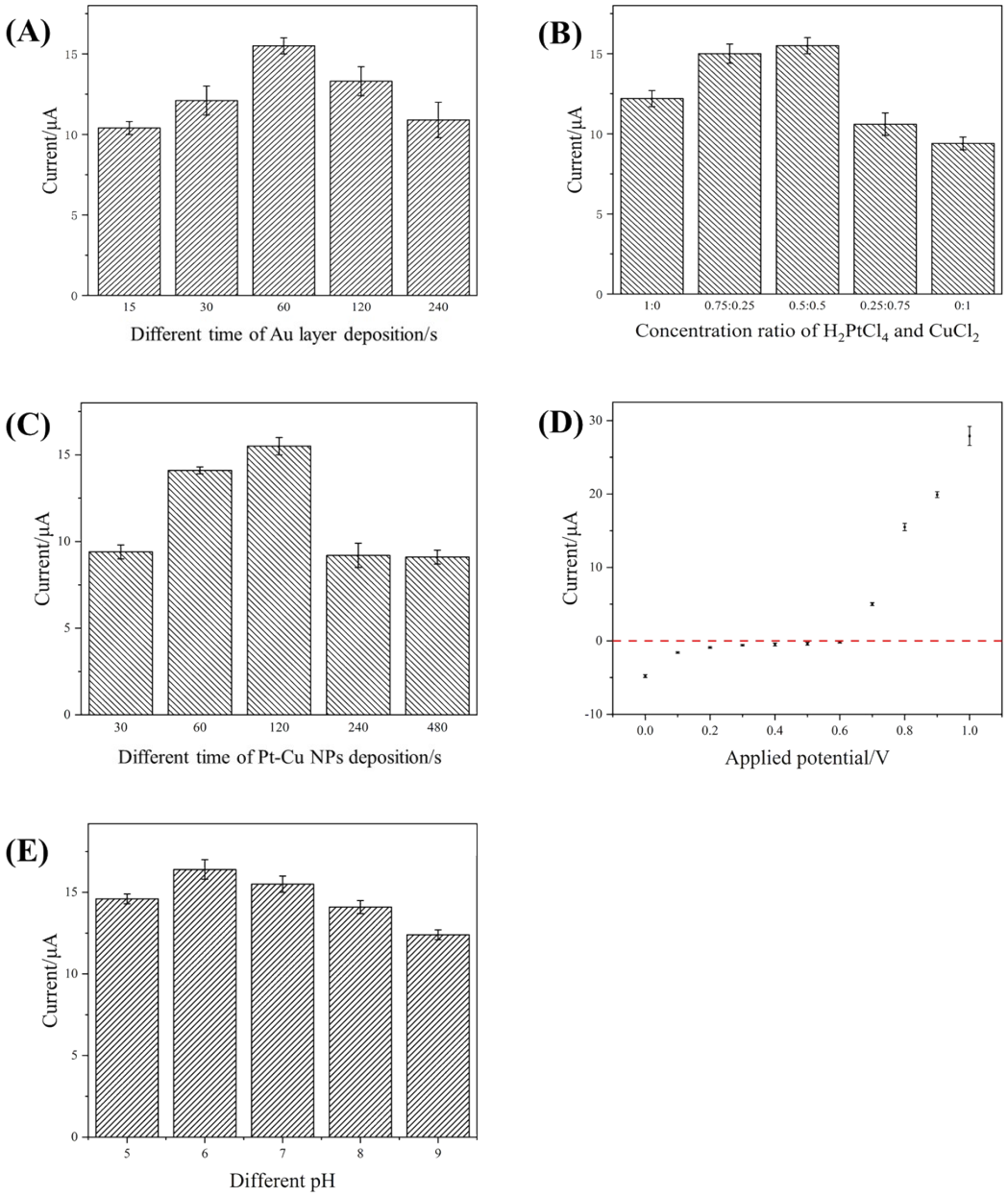

Fig. S5 Optimization of the Pt–Cu NPs and Au underlayer for amperometric detection of 1 mM $NaNO_2$: (A) Influence of Au electrodeposition time on the amperometric current. (B) Influence of the molar ratio between H_2PtCl_6 and $CuCl_2$ on the amperometric current. (C) Influence of the deposition duration of Pt–Cu NPs on the amperometric current. (D) Influence of working potential on the amperometric current. (E) Influence of solution pH on the amperometric current.

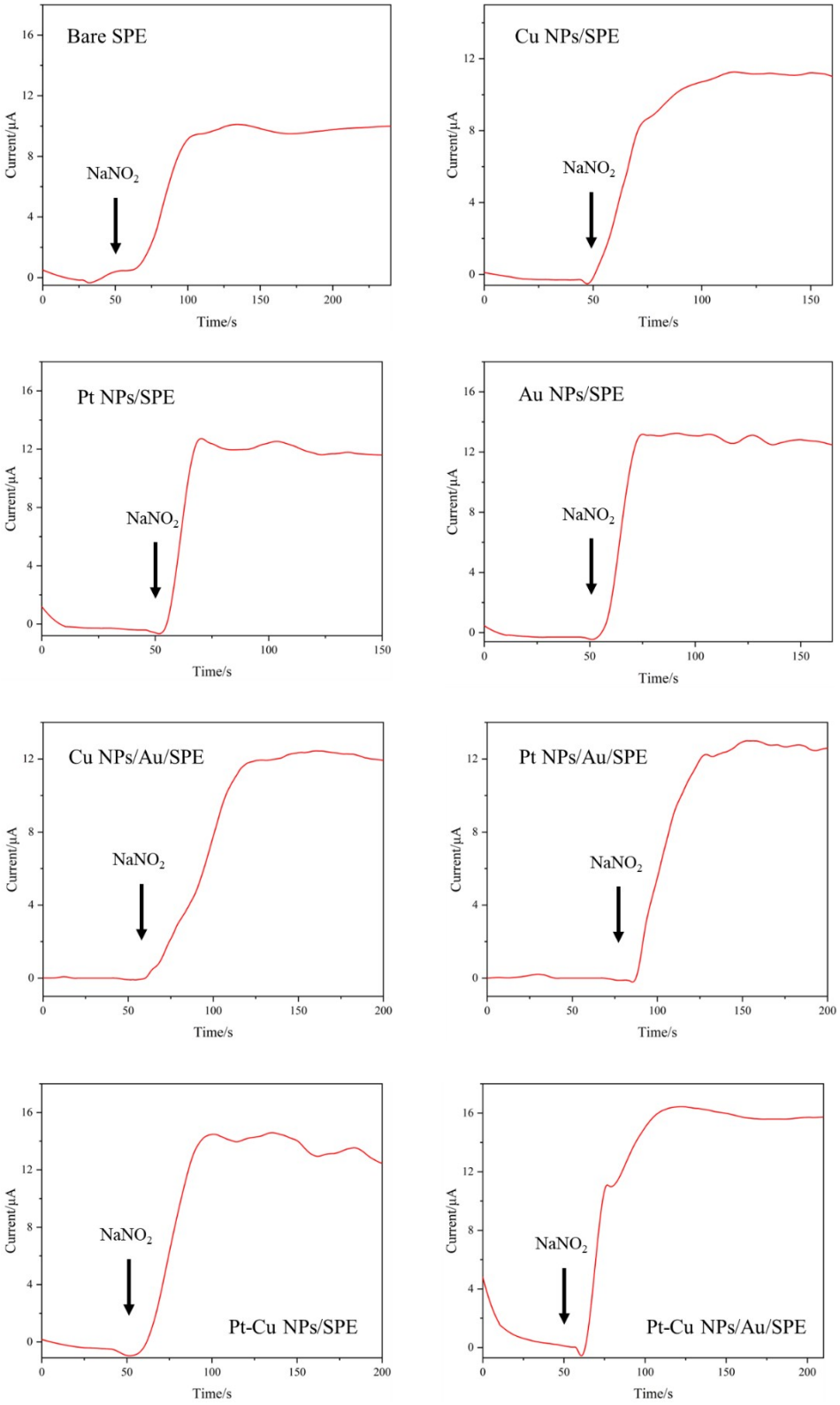

Fig. S6 The amperometric responses of bare SPE, Cu NPs/SPE, Pt NPs/SPE, Au NPs/SPE, Cu NPs/Au/SPE, Pt NPs/Au/SPE, Pt-Cu NPs/SPE and Pt-Cu NPs/Au/SPE in 1 mM $NaNO_2$.

Table S1 Comparison of electroactive surface area, nitrite oxidation current, and normalized current density for different electrodes.

Electrode	EASA (cm^2)	$I_{nitrite}$ (μA)	Normalized current density ($μA \cdot cm^{-2}$)
Bare SPE	0.0897	9.7	108.1
Au NPs/SPE	0.1031	11.6	112.5
Pt NPs/SPE	0.1134	12.6	111.1
Cu NPs/SPE	0.1007	11.1	110.2
Pt–Cu NPs/SPE	0.1138	13.2	116.0
Pt NPs/Au/SPE	0.1126	12.7	112.8
Cu NPs/Au/SPE	0.1085	12.1	111.5
Pt–Cu NPs/Au/SPE	**0.1197**	**15.5**	**129.5**

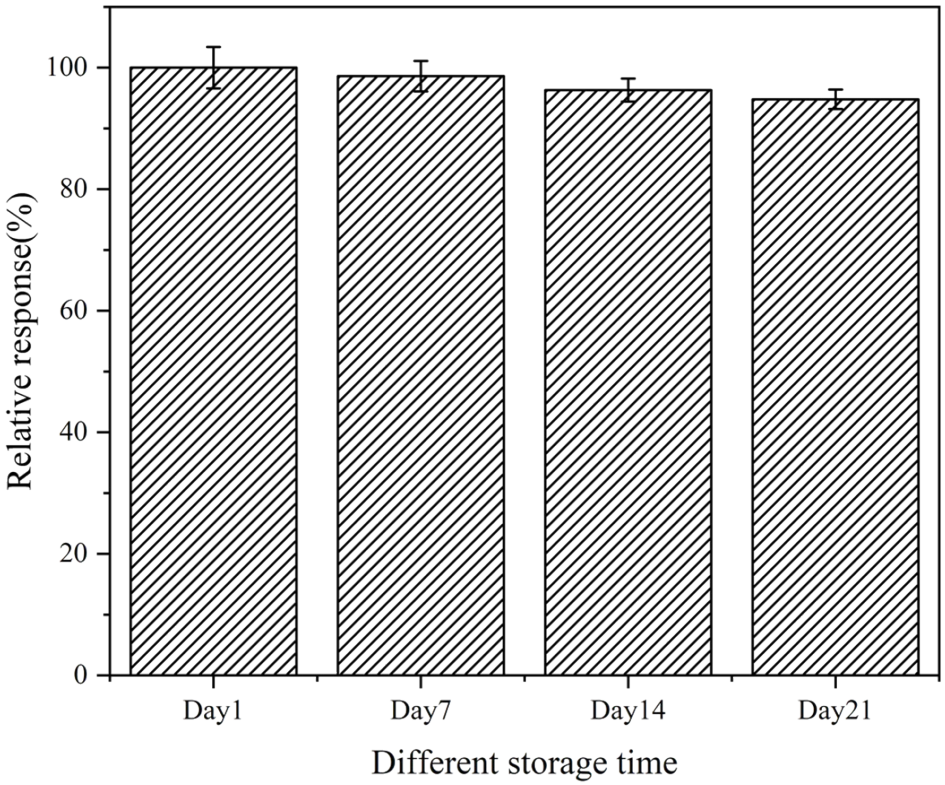

Fig. S7 Storage stability showing relative current response of Pt-Cu NPs/Au/SPE to 1 mM $NaNO_2$ solution over time.

Table S2. Comparison between different electrochemical nitrite sensors

Sensor	Sensor type	Potential	Linear range (μM)	LOD (μM)	Sensitivity (μA·mM·cm^{-2})	Ref
1	Pt NPs/ErGO/GCE	+0.75 V	5-1000	0.22	—	[1]
2	Cu−Co oxide/rGO/GCE	+0.75 V	100-2800	0.5	74.36	[2]
3	PM/AuNPs/MWCNTs/GCE	+0.73 V	0.4-1475	0.041	—	[3]
4	Pt@ApoF/Ti_3C_2/GCE	+0.8 V	1-9000	0.425	—	[4]
5	Pt NPs/MWCNTs/GCE	+0.8 V	4-2400	1.50	40.60	[5]
6	Au NRs/ErGO/PEDOT:PSS/GCE	—	0.8-100	0.20	637.90	[6]
7	Cu-MOF/Au	+0.8 V	0.1-4000	0.082	17.00	[7]
8	Ag/Cu/MWNTs/GCE	+0.8 V	1-1000	0.20	380.90	[8]
9	Cu Nanoplates/GCE	+1.25 V	0-5000	8.90	37.58	[9]
10	**Pt-Cu NPs/Au/SPE**	**+0.8 V**	**1-7500**	**0.11**	**226.03**	**This work**

ErGO: electrochemical reduction of graphene oxide; GCE: glassy carbon electrode; rGO: reduced graphene oxide; PM: poly-melamine; ApoF: apoferritin; MWCNTs: multiwall carbon nanotubes; Au NRs: gold nanorods.

Table S3 Cost breakdown per sensor unit.

Material	Consumption	Unit Price	Cost ($)
Au	10 μM	$11.4 per mM	0.11
Pt	20 μM	$25.8 per mM	0.52
Cu	20 μM	$4.3 per mM	0.09
Carbon paste	1 g	$0.05 per g	0.05
PET board	1/28 per	$0.14 per	0.005
Salinometer	1 per	$0.018 per	0.018
Total			≈ 0.80

Table S4. Recovery and relative standard deviation for nitrite detection in spiked real-world samples. The salinity (NaCl concentration) was measured using a commercial salinometer.

Sample No.	Actual samples	Salinity （M）	Added （μM）	Measured value （μM）	Recovery （%）	RSD （%）
1	Water	0	10	9.83±0.15	98.31±1.51	1.49
2	Water	0	50	50.83±1.72	101.67±3.44	3.39
3	Water	0	100	102.50±3.62	102.50±3.62	3.53
4	Cola	0.01	10	9.93±0.21	99.37±2.15	2.13
5	Cola	0.01	50	48.51±0.98	97.01±1.96	2.02
6	Cola	0.01	100	102.01±1.81	102.01±1.81	1.77
7	Milk	0.04	10	10.03±0.12	100.31±0.24	1.2
8	Milk	0.04	50	49.51±0.95	99.03±1.90	1.92
9	Milk	0.04	100	96.43±1.60	96.43±1.60	1.66
10	River water	0.01	10	9.81±0.14	98.12±1.45	1.39
11	River water	0.01	50	51.18±1.02	102.37±2.04	1.99
12	River water	0.01	100	103.75±1.19	103.75±1.19	1.15
13	Pickled ginger	0.22	10	5.66±0.28	56.62±2.84	5.01
14	Pickled ginger	0.22	50	40.09±0.63	80.18±0.43	0.54
15	Pickled ginger	0.21	100	84.00 ± 2.85	84.00±2.85	3.40
16	Pickled Chinese onion	0.47	10	4.37±0.15	43.71±1.54	3.34
17	Pickled Chinese onion	0.48	50	33.58±1.38	67.16±2.76	4.10
18	Pickled Chinese onion	0.47	100	64.72 ± 1.59	64.72±1.59	2.45
19	Pickled garlic cloves	0.44	10	6.45±0.17	62.30±6.30	2.68
20	Pickled garlic cloves	0.44	50	21.89±0.74	43.79±1.47	3.36
21	Pickled garlic cloves	0.43	100	62.88±3.36	62.88±3.36	5.34
22	Pickled baby mustard	0.42	10	5.64±0.16	56.44±1.62	2.87
23	Pickled baby mustard	0.43	50	32.38±0.94	64.76±1.88	2.90
24	Pickled baby mustard	0.43	100	56.18 ± 2.59	56.18±2.59	4.62

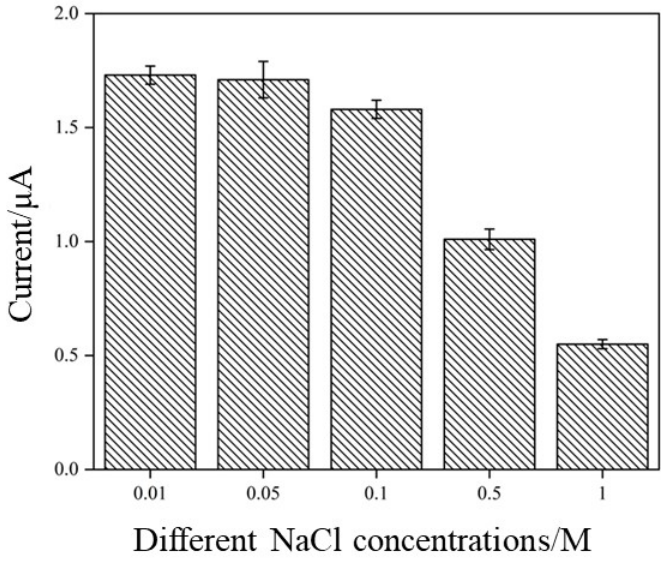

Fig. S8 Effect of different concentrations of NaCl on the current response of the Pt-Cu NPs/Au/SPE toward 1 mM nitrite.

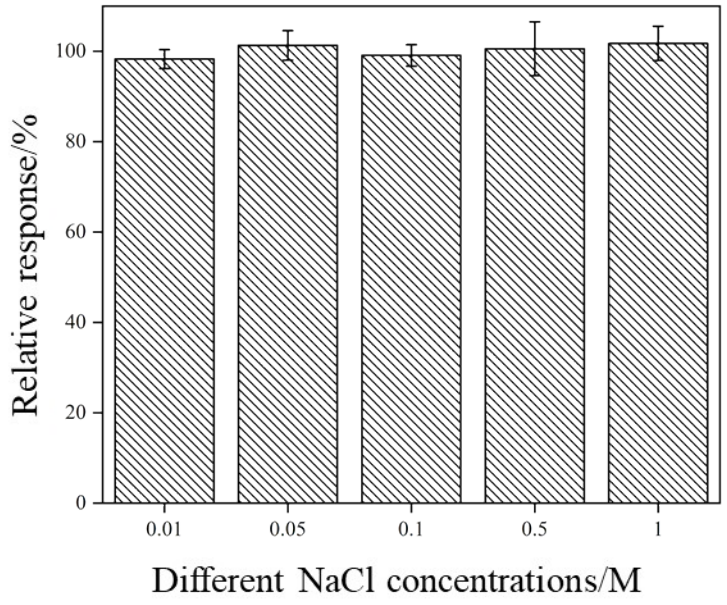

Fig. S9. Recovery performance of the AI-compensated sensor for 1 mM nitrite across different NaCl concentrations (0.01-1 M).

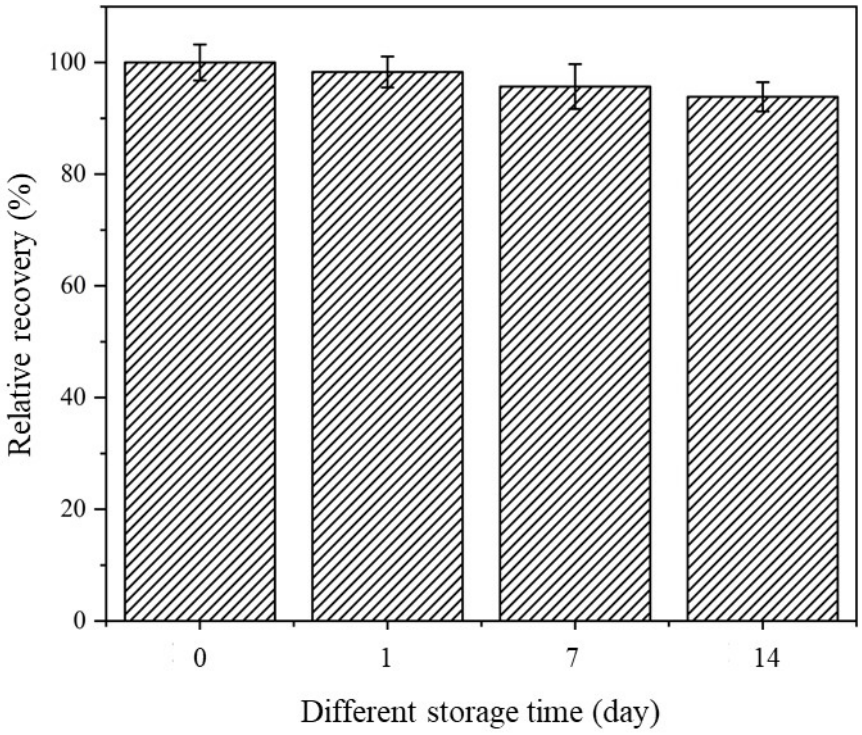

Fig. S10 Operational stability of the Pt–Cu NPs/Au/SPE sensor in food matrix. The relative recovery of nitrite concentration is shown over a 14-day period during repeated testing in a pickled ginger sample spiked with 50 μM $NaNO_2$ using the same batch of electrodes.

Reference

(1) Vijayaraj, K.; Jin, S. H.; Park, D. S. A Sensitive and Selective Nitrite Detection in Water Using Graphene/Platinum Nanocomposite. *Electroanalysis* **2016**, *29* (2), 345-351. DOI: 10.1002/elan.201600133.

(2) Ma, J. x.; Ning, Y.; Yang, L.; Feng, Y.; Liu, Y. Preparation of reduced graphene oxide decorated with Cu-Co Oxide Electrode and its application for Sensitive Determination of Nitrite in Food Samples. *International Journal of Electrochemical Science* **2021**, *16* (12). DOI: 10.20964/2021.12.53.

(3) Han, E.; Li, L.; Gao, T.; Pan, Y.; Cai, J. Nitrite determination in food using electrochemical sensor based on self-assembled MWCNTs/AuNPs/poly-melamine nanocomposite. *Food Chemistry* **2024**, *437*. DOI: 10.1016/j.foodchem.2023.137773.

(4) Mu, R.; Zhu, D.; Wei, G. Ti3C2 Nanosheets Functionalized with Ferritin–Biomimetic Platinum Nanoparticles for Electrochemical Biosensors of Nitrite. *Biosensors* **2024**, *14* (5). DOI: 10.3390/bios14050258.

(5) Etesami, M.; Mohamed, N. Preparation of Pt/MWCNTs Catalyst by Taguchi Method for Electrooxidation of Nitrite. *Journal of Analytical Chemistry* **2016**, *71* (2), 185-194. DOI: 10.1134/s1061934816020040.

(6) Wahyuni, W. T.; Rahman, H. A.; Afifah, S.; Anindya, W.; Hidayat, R. A.; Khalil, M.; Fan, B.; Putra, B. R. Comparison of the analytical performance of two different electrochemical sensors based on a composite of gold nanorods with carbon nanomaterials and PEDOT:PSS for the sensitive detection of nitrite in processed meat products. *RSC Adv.* **2024**, *14* (34), 24856-24873. DOI: 10.1039/d4ra04629c.

(7) Zhao, X.; Zhou, G.; Qin, S.; Zhang, J.; Wang, G.; Gao, J.; Suo, H.; Zhao, C. In Situ Preparation of Metallic Copper Nanosheets/Carbon Paper Sensitive Electrodes for Low-Potential Electrochemical Detection of Nitrite. *Sensors* **2024**, *24* (13). DOI: 10.3390/s24134247.

(8) Zhang, Y.; Nie, J.; Wei, H.; Xu, H.; Wang, Q.; Cong, Y.; Tao, J.; Zhang, Y.; Chu, L.; Zhou, Y.; et al. Electrochemical detection of nitrite ions using Ag/Cu/MWNT nanoclusters electrodeposited on a glassy carbon electrode. *Sens. Actuators B Chem.* **2018**, *258*, 1107-1116. DOI: 10.1016/j.snb.2017.12.001.

(9) Liu, X.; Li, Y.; Yang, W.; Sun, X. Surfactant-free synthesis of 2D Cu nanoflakes as electrochemical sensors and their applications for detection of formaldehyde, nitrite and glucose. *Journal of Food Composition and Analysis* **2024**, *131*. DOI: 10.1016/j.jfca.2024.106245.